[2]Johari, H., Olinger, D. J., and Fitzpatrick, K. C., "Delta Wing Vortex Control via Recessed Angled Spanwise Blowing," *Journal of Aircraft*, Vol. 32, No. 4, 1995, pp. 804–810.

[3]Wong, G. S., Rock, S. M., Wood, N. J., and Roberts, L., "Active Control of Wing Rock Using Tangential Leading-Edge Blowing," *Journal of Aircraft*, Vol. 31, No. 3, 1994, pp. 659–665.

[4]Pedreiro, N., Rock, S. M., Celik, Z. Z., and Roberts, L., "Roll–Yaw Control at High Angle of Attack by Forebody Tangential Blowing," *Journal of Aircraft*, Vol. 35, No. 1, 1998, pp. 69–77.

[5]Sreenatha, A. G., and Ong, T. K., "Wing Rock Suppression Using Recessed Angle Spanwise Blowing," *Journal of Aircraft*, Vol. 39, No. 5, 2002, pp. 900–903.

[6]Nayfeh, A. H., Elzebda, J. M., and Mook, D. T., "Development of an Analytical Model of Wing Rock for Slender Delta Wings," *Journal of Aircraft*, Vol. 26, No. 8, 1989, pp. 737–743.

[7]Nayfeh, A. H., Elzebda, J. M., and Mook, D. T., "Analytical Study of Subsonic Wing Rock Phenomenon for Slender Delta Wings," *Journal of Aircraft*, Vol. 26, No. 9, 1989, pp. 805–809.

[8]Sreenatha, A. G., and Lim, Y., "Stability and Robustness Analysis of Fuzzy Logic Controller for Wing Rock Suppression," *AIAA Atmospheric Flight Mechanics Conference*, AIAA Reston, VA, 2000, pp. 701–706.

[9]Joshi, S. V., Sreenatha, A. G., and Chandrasekhar, J., "Suppression of Wing Rock of Slender Delta Wings Using a Single Neuron Controller," *IEEE Transactions on Control Systems Technology*, Vol. 6, No. 5, 1998, pp. 671–677.

[10]Chang, W., Joo, Y. H., Pak, J. B., and Chen, G., "Robust Fuzzy-Model-Based Controller for Uncertain Systems," *1999 IEEE International Fuzzy Systems Conference Proceedings*, IEEE Press, Piscataway, NJ, 1999, pp. 486–491.

[11]Venayagamoorthy, G. K., and Harley, R. G., "A Robust Artificial Neural Network Controller for a Turbogenerator when Line Configuration Changes," *Proceedings of the IEEE Africon'99 Conference*, Vol. 2, IEEE Press, Piscataway, NJ, 1999, pp. 917–922.

Transpiration Boundary Condition for Computational Fluid Dynamics Solutions in Noninertial Reference Frames

Timothy J. Cowan,* Charles R. O'Neill,† and Andrew S. Arena Jr.‡
Oklahoma State University, Stillwater, Oklahoma 74078

Nomenclature

$\boldsymbol{n}$	=	surface normal vector
$\boldsymbol{n}'$	=	deformed surface normal vector
$\boldsymbol{r}$	=	position vector
$\boldsymbol{u}$	=	fluid velocity vector
$\boldsymbol{V}_b$	=	boundary surface velocity vector
$\Delta\boldsymbol{r}$	=	deformation vector
Ω	=	angular velocity matrix

Introduction

THE practicality of time-marched computational fluid dynamics (CFD) solutions for the prediction of aeroelastic and aeroservoelastic characteristics has progressed significantly due to continued advancement in computational capability. Such solutions involve the use of Euler or Navier–Stokes fluid dynamic algorithms coupled with a structural dynamics algorithm through boundary conditions. Unfortunately, the solution computational time increases dramatically if the computational domain must be rediscretized to account for moving structural boundary surfaces. The added computational time and the complexity associated with the meshing process diminish the attractiveness of the approach for full aircraft configurations or other applications where a more rapid 'turnaround' is required, such as flight-test support. Although moving meshes and other methodologies such as grid rediscretization are excellent approaches to problems that are not amenable to small-disturbance assumptions, many problems of practical interest are dominated by mean-flow conditions, under which body motions may be represented by small surface perturbations.

Hence, a method of simulating the boundary deformations for the CFD solver, without actually deforming the computational domain, has proven to be an efficient tool for unsteady aeroelastic predictions. A number of references have demonstrated the viability of this approach, known as the transpiration method, for a wide variety of ploblems.[1–9] The transpiration method was first developed by Lighthill to simulate changes in airfoil thickness.[1] Lighthill modified the normal velocity just outside the boundary layer of an airfoil using the method of equivalent sources to simulate the effects of the boundary layer. This technique has also been used for boundary-layer patching with inviscid-flow techniques. More recently, the technique has been used to simulate surface deformation in full potential solution techniques and in steady and unsteady Euler codes.[2–9]

This Note outlines an extension of the basic transpiration approach and applies the method to problems that are cast in a noninertial frame. This extension of the problem allows a significantly larger set of practical problems to be modeled in this manner because unsteady structural and control deflections may be modeled on geometries undergoing large-amplitude motions. Examples include aeroelasticity, aeroservoelasticity of aircraft undergoing large-amplitude flight dynamics maneuvers, and vibration and aeroelastic modeling of propellers, helicopter rotors, and fans.

Inertial Transpiration

For an aeroelastic CFD solution, the deformed state of the structure is typically defined by a set of structural mode shapes. The mode shapes define a deformation vector for every surface node in the computational domain. Consider the deformed state given by Fig. 1, where the two nodes of an edge have been displaced from their initial position by a deformation vector $\Delta\boldsymbol{r}$.

In a CFD solution, this statically deformed shape can be simulated, without actually deforming the surface grid, by using the deformed normal vector $\boldsymbol{n}'$ when enforcing flow tangency. The original

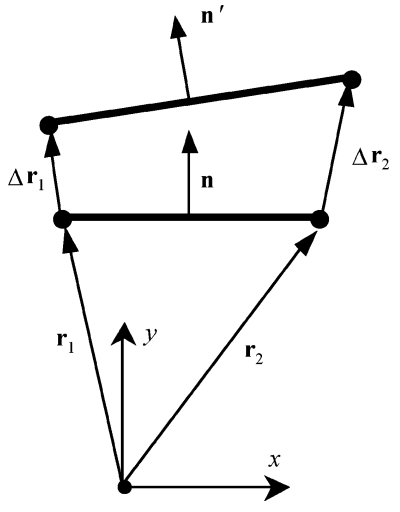

Fig. 1 Illustration of transpiration concept.

Received 5 December 2003; accepted for publication 20 January 2004.

*Aerospace Engineer. Member AIAA.

†Graduate Research Assistant, Mechanical and Aerospace Engineering. Student Member AIAA.

‡L. Andrew Maciula Professor, Mechanical and Aerospace Engineering Department. Senior Member AIAA.

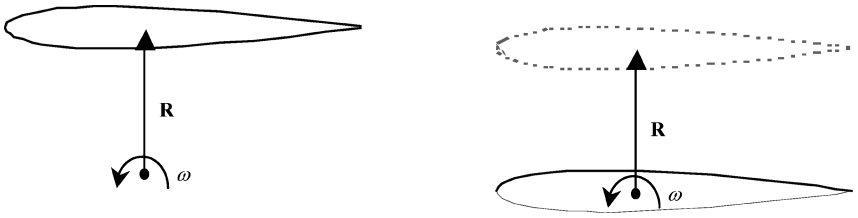

Fig. 2 Model problem for testing transpiration with noninertial rotation.

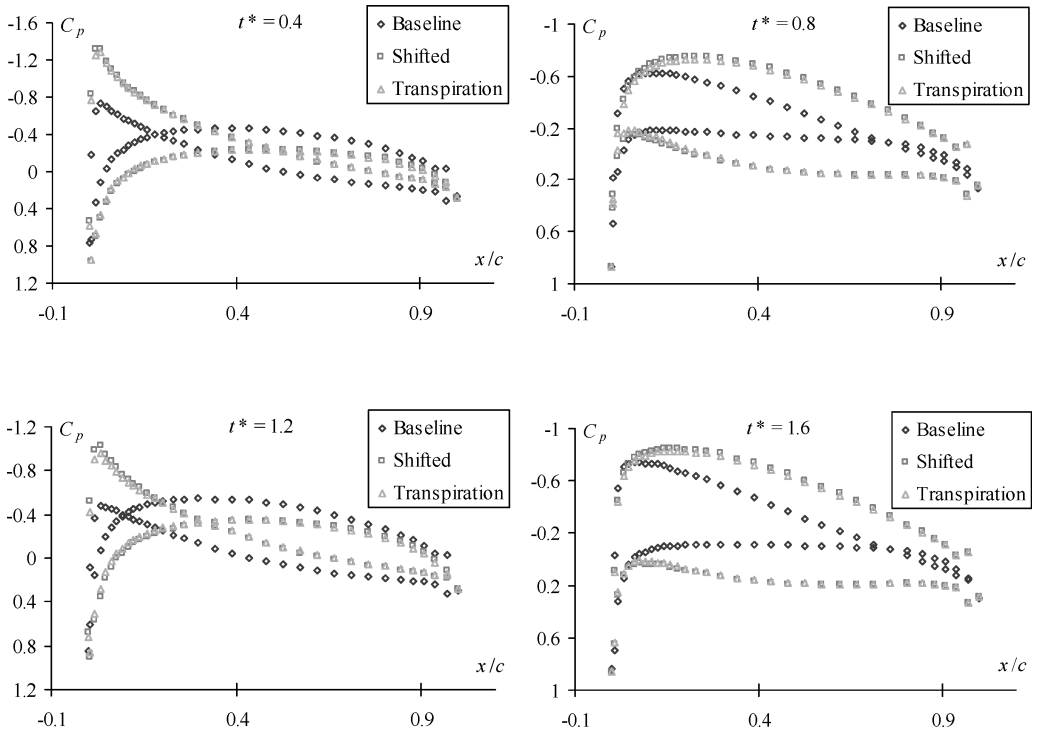

Fig. 3 Comparison of predicted pressure coefficients for a pitching airfoil.

normal vector is used to evaluate the boundary integral and maintain flux conservation, but flow tangency at each wall node is enforced based on the deformed shape of the structure. This results in a situation where the normal component of the fluid velocity on the wall surfaces is no longer necessarily zero because the flow is forced to follow the deformed shape of the surface.

In addition to statically deformed structures, it is necessary to simulate dynamically deforming structures for an aeroelastic simulation. In this case, the elastic surface is continuously changing its deformed shape and has an associated deformation velocity $\boldsymbol{V}_b$ for each node on the boundary. The transpiration boundary condition for a node on a dynamically deforming solid wall is

$$\boldsymbol{u} = \boldsymbol{u} - (\boldsymbol{u} \cdot \boldsymbol{n}' - \boldsymbol{V}_b \cdot \boldsymbol{n}')\boldsymbol{n}' \tag{1}$$

Equation (1) simply ensures that the normal component of the fluid velocity is equal to the normal component of the boundary velocity at each node, using the deformed normal vector.

Noninertial Transpiration

Research has demonstrated that CFD results that are obtained employing the inertial-transpiration boundary condition are in excellent agreement with those obtained using actually deformed grids for the small deformations typically seen in aeroelastic simulations.[10] However, it is not expected that this methodology will accurately represent a deformed body in a noninertial frame. Consider the two cases illustrated in Fig. 2.

The graphic on the left in Fig. 2 represents an airfoil in a rotating frame of reference with the origin of rotation a vector distance $\boldsymbol{R}$ away from the midpoint of the airfoil, whereas the graphic on the right is attempting to simulate the same rotating airfoil using transpiration to shift an airfoil rotating about its midpoint to the vector location $\boldsymbol{R}$. Obviously, these two problems are very different unless the transpiration method accurately accounts for the noninertial rotation of the shifted body. However, the transpiration procedure presented so far would effectively do nothing because the body has been shifted uniformly, with no change in surface normals, to a new static position.

Consider what would happen if we rotated the coordinate system illustrated in Fig. 1. In this case, the velocity for either of the two nodes of the boundary element is given by the following equation:

$$\boldsymbol{V}_{b,i} = \boldsymbol{\Omega}(\boldsymbol{r}_i + \Delta\boldsymbol{r}_i) = \boldsymbol{\Omega}\boldsymbol{r}_i + \boldsymbol{\Omega}\Delta\boldsymbol{r}_i \tag{2}$$

Because we are simulating elastic deformation using transpiration, it will be necessary to account for the $\Omega\Delta\boldsymbol{r}$ term in the transpiration boundary condition. This term will simply be treated as an additional boundary velocity for each node, giving us the following equation for our solid-wall boundary condition:

$$\boldsymbol{u} = \boldsymbol{u} - [\boldsymbol{u} \cdot \boldsymbol{n}' - (\boldsymbol{V}_b + \boldsymbol{\Omega}\Delta\boldsymbol{r}) \cdot \boldsymbol{n}']\boldsymbol{n}' \tag{3}$$

Equation (3) now simulates the elastic deformations for a solid-wall boundary in either an inertial or a noninertial frame of reference.

Results

As a simple verification of this noninertial transpiration methodology, consider the airfoil illustrated in Fig. 2, where the displacement vector $\boldsymbol{R}$ is oriented in the negative x direction with a magnitude

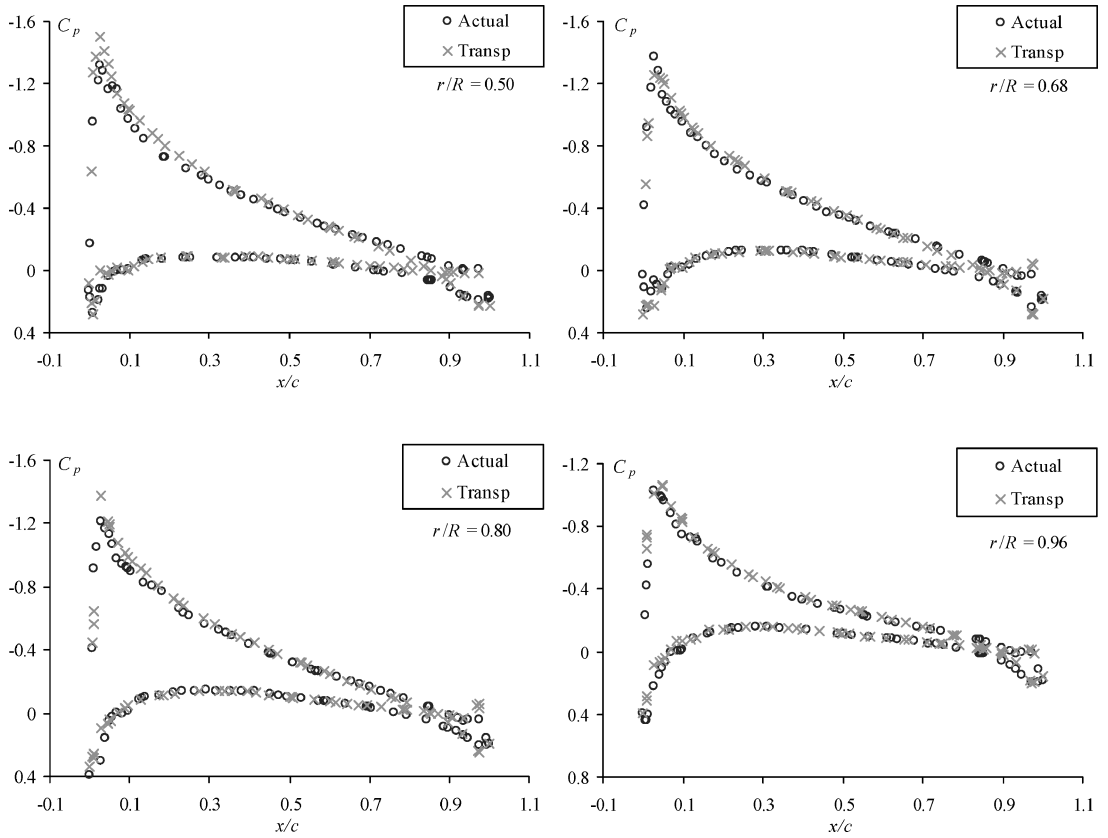

Fig. 4 Comparison of computed surface-pressure distributions for a hovering rotor.

equal to half the chord of the airfoil. The displacement vector is $\boldsymbol{R} = (-\frac{1}{2}c, 0)$. This puts the origin of rotation at the trailing edge of the airfoil. The airfoil is then forced into an oscillating pitch motion with a dimensionless frequency of $\omega^* = 2.0$, where the dimensionless frequency is defined as follows:

$$\omega^* = \omega c / 2U_\infty \tag{4}$$

Three different simulations are performed for this airfoil. First, a baseline solution is run for a noninertial solution with the airfoil pitching at its midpoint. Second, a "shifted" solution is run for a noninertial solution with the pitch location shifted a distance $\boldsymbol{R}$ from the midpoint. Finally, a transpiration solution is run for a noninertial solution with the airfoil pitching about its midpoint, with a simulated shift to the location $\boldsymbol{R}$ using the transpiration method corrected for a rotating noninertial frame. Figure 3 compares the surface-pressure distributions predicted by these three solutions at four different instants in time.

Notice that the shifted and transpiration solutions are in excellent agreement even for this relatively large displacement. The baseline solution is presented only to show that the shifted axis has a significant effect on the resulting pressure distributions. Thus, we see that without the noninertial correction to the transpiration method, we would have a significantly inaccurate representation for the shifted noninertial solution.

As a more significant validation of noninertial transpiration, we investigate the unsteady dynamics of a hovering rotor. This type of flow problem is considered suitable for Euler codes because the essential physics is expected to be inviscid and separation typically does not occur.[11] The geometry for this problem is the two-bladed rotor used in the experiments of Caradonna and Tung.[12] Since the publication of their original experimental results, this rotor has been the basis of numerous computational simulations ranging from panel methods[13] to fully three-dimensional CFD solutions.[14,15] One might even consider this to be the standard validation case for a noninertial CFD solution, considering the wealth of computational data that are available for it.

The geometry used in this study was a rotor consisting of two cantilever-mounted, rectangular blades with NACA 0012 cross sections. The blades are untwisted and untapered, with an aspect ratio of 6 and a precone of 0.5 deg. The total diameter of the rotor disk is 7.5 ft, the chord of the blades is 0.625 ft, and the cutout radius at the center of the rotor is equal to one chord. The rotor is positioned in the computational domain so that two-thirds of the volume is below the plane of the rotor. This volume below the rotor captures the unsteady wake that develops. The computational grid generated for this study consists of approximately 1.5 million elements. For accurate representation of the wake, the highest element density is in the region below the plane of the rotor. Initial tests with fewer elements showed that the wake was not accurately modeled, and the problem behaved more like a simple rectangular wing in a linearly varying velocity field.

The test solution is for a hover case with a collective pitch angle of 8 deg and a tip Mach number of 0.439. The collective pitch angle of the rotor can be represented by actual rotation of the blades or by simulating the rotation using transpiration on a baseline rotor model with zero pitch. Figure 4 presents computed surface-pressure results for both the actual rotation case and the transpiration case. The results shown are for the fully converged case following approximately eight revolutions of the rotor. For our purposes, the primary comparison for both of these solutions is between the two sets of computational results.

Conclusions

An extension to the basic transpiration method for modeling steady and unsteady perturbations in surface geometries in CFD solutions has been presented. It has been shown that this method is viable and is particularly attractive for a wide range of practical problems for which surface motion may be represented as a perturbation on a body undergoing even a relatively large-amplitude noninertial rotational motion.

Acknowledgments

Funds for the support of this study have been provided by the NASA Dryden Flight Research Center, Oklahoma State University, and the Oklahoma Space Grant Consortium.

References

[1]Lighthill, M. J., "On Displacement Thickness," *Journal of Fluid Mechanics*, Vol. 4, Pt. 4, Jan. 1958, pp. 383–392.

[2]Sankar, N. L., Malone, J. B., and Tassa, Y., "An Implicit Conservative Algorithm for Steady and Unsteady Three-Dimensional Transonic Potential Flows," AIAA Paper 81-1016, June 1981.

[3]Sankar, N. L., Ruo, S. Y., and Malone, J. B., "Application of Surface Transpiration in Computational Aerodynamics," AIAA Paper 86-0511, Jan. 1986.

[4]Sankar, N. L., Malone, J. B., and Schuster, D., "Euler Solutions for Transonic Flow past a Fighter Wing," *Journal of Aircraft*, Vol. 24, No. 1, 1987, pp. 10–16.

[5]Bharadvaj, Bala, K., "Computation of Steady and Unsteady Control Surface Loads in Transonic Flow," AIAA Paper 90-0935, 1990.

[6]Raj, P., and Harris, B., "Using Surface Transpiration with an Euler Method for Cost-Effective Aerodynamic Analysis," AIAA Paper 93-3506, Aug. 1993.

[7]Fisher, C. C., and Arena, A. S., "On the Transpiration Method for Efficient Aeroelastic Analysis Using an Euler Solver," AIAA Paper 96-3436, July 1996.

[8]Stephens, C. H., and Arena, A. S., "Application of the Transpiration Method for Aeroservoelastic Prediction Using CFD," AIAA Paper 98-2071, April 1998.

[9]Stephens, C. H., and Arena, A. S., "CFD-Based Aeroservoelastic Predictions with Comparisons to Benchmark Experimental Data," AIAA Paper 99-0766, Jan. 1999.

[10]Cowan, T. J., "Finite Element CFD Analysis of Super-Maneuvering and Spinning Structures," Ph.D. Dissertation, Oklahoma State Univ., May 2003.

[11]Caradonna, F. X., and Tung, C., "Finite-Difference Computations of Rotor Loads," NASA TM 86682, April 1985.

[12]Caradonna, F. X., and Tung, C., "Experimental and Analytical Studies of a Helicopter Rotor in Hover," NASA TM 81232, Sept. 1981.

[13]Katz, J., and Maskew, B., "Unsteady Low-Speed Aerodynamic Model for Complete Aircraft Configurations," *Journal of Aircraft*, Vol. 25, No. 4, 1988, pp. 302–310.

[14]Yang, G., and Zhuang, L., "Numerical Simulation of Rotor Flow in Hover," *Journal of Aircraft*, Vol. 37, No. 2, 2000, pp. 221–226.

[15]Modi, A., Sezer-Uzol, N., Long, L. N., and Plassmann, P. E., "Scalable Computational Steering System for Visualization of Large-Scale CFD Simulations," AIAA Paper 2002-2750, June 2002.